Z. Phys. B – Condensed Matter 71, 355–368 (1988)

Condensed
Zeitschrift für Physik B Matter

On the critical dynamics of ferromagnets

E. Frey and F. Schwabl
Institut für Theoretische Physik,
Physik-Department der Technischen Universität München, Garching,
Federal Republic of Germany

Received December 24, 1987

The dynamic scaling functions for ferromagnets above and below the critical temperature are determined using mode coupling theory. Below the critical temperature we study isotropic ferromagnets taking into account the exchange interaction only and give the first numerical solution of the resulting mode coupling equations. In the paramagnetic phase we examine how the critical dynamics is modified by the addition of the dipole-dipole interaction. On the basis of this theory we are able to explain in a unifying fashion the results of different experimental methods; i.e.: neutron scattering, hyperfine interaction and electron-spin resonance. Predictions for new experiments are made.

1. Introduction

Ferromagnets in the vicinity of their Curie point were among the first systems where critical dynamical phenomena with nonclassical features were observed experimentally. Theoretically a qualitative and increasingly quantitative understanding was provided by dynamical scaling theory, mode coupling and the renormalization group theory. In the region where the exchange interaction dominates, the mode coupling theory was particularly successful for isotropic Heisenberg ferromagnets.

In the following we extend the mode coupling theory for isotropic exchange ferromagnets to the ferromagnetically ordered phase and include dipole-dipole forces in the paramagnetic phase. In the ordered phase we disregard dipolar forces. Hence the longitudinal and transverse scaling functions can be viewed as the analogues of the Resibois-Piette scaling function [1] for the paramagnetic phase. Clearly this part of our theory can be applied only to experiments not too close to T_c and for not too small wave vectors such that dipolar forces are negligible. Nevertheless it should allow to interpret and stimulate experiments below the Curie point.

In order to avoid confusion we draw attention to the different connotation of the terms transverse and longitudinal. For the isotropic ferromagnet below T_c these refer to the direction of the magnetization, while for the dipolar ferromagnet they refer to the direction of the wave vector.

Concerning the importance of the dipolar forces we note. Because of the long range character of the dipole-dipole interaction it dominates the critical behaviour in the immediate vicinity of the critical point and for small wavevectors. If the dipolar interaction is weak compared to the exchange interaction there is a crossover from isotropic critical behaviour to dipolar critical behaviour [2]. The static crossover can be characterised by a wave vector q_D. It turns out that the static critical exponents of the dipolar fixed point are very close to the isotropic [2]. The most significant crossover can be seen in the longitudinal susceptibility, which is equal to the transverse susceptibility for ξ^{-1} and $q \gg q_D$ and remains finite in the opposite limit. Here ξ is the correlation length and q the wave number. A widely held expectation was that also the dynamic quantities should show a crossover at q_D. Indeed this crossover was found in the local relaxation time in NMR experiments. On the other hand in neutron scattering experiments the dynamic crossover could not be detected. Right at T_c the critical behaviour was found to be isotropic down to almost a tenth of q_D. What made the situation even more bewildering was the fact that nevertheless neutron scattering data could not be fitted by

the Resibois-Piette scaling function. Recently the authors have developed a mode coupling theory for dipolar ferromagnets [3], on the basis of which one can explain the seemingly conflicting features of neutron scattering. Here we expose our theory in more detail and apply it to two more groups of experiments; i.e. local experiments as NMR characterised by the local relaxation rate and to electron spin resonance (ESR).

The outline of the paper is as follows: In the rest of the introductory section we briefly describe the general structure of mode coupling equations. In Sect. 2 we review the mode coupling theory for isotropic ferromagnets with pure exchange interaction above and below the critical temperature. Furthermore we will give a numerical solution of the mode coupling equations below the critical temperature. In Sect. 3 we derive the mode coupling equations for ferromagnets with both short range exchange and long range dipolar interactions in the paramagnetic phase. We apply the theory to neutron scattering, NMR and ESR experiments. In the final Chap. 4 we summarize the results and propose further experiments.

Now we give a brief outline of the general structure of mode coupling equations. The quantity of interest is the Kubo relaxation matrix for the dynamical variables $\{X^\alpha(\mathbf{q})\}$, which is defined by

$$\Phi^{\alpha\beta}(q,\omega)=\int_0^\infty \mathrm{d}t\, \mathrm{e}^{\mathrm{i}\omega t}\Phi^{\alpha\beta}(q,t) \tag{1.1}$$

with

$$\Phi^{\alpha\beta}(q,t)=i\lim_{\varepsilon\to 0}\int_t^\infty \mathrm{d}\tau\, \mathrm{e}^{-\varepsilon\tau}\langle[X^\alpha(\mathbf{q},\tau), X^\beta(\mathbf{q},0)^\dagger]\rangle, \tag{1.2}$$

where the dynamical variables are normalized with respect to the static susceptibility $\chi^{\alpha\beta}\equiv(X^\alpha, X^\beta)=\delta^{\alpha\beta}$. Using a Mori projection formalism [4] one finds a generalized Langevin equation, which in terms of the Kubo relaxation matrix can be written as follows

$$\Phi^{\alpha\beta}(q,\omega)=\left(\frac{1}{\omega-C(q)+i\Gamma(q,\omega)}\right)^{\alpha\beta}. \tag{1.3}$$

The frequency matrix $C^{\alpha\beta}(q)$ is given by

$$C^{\alpha\beta}(q)=\frac{1}{\hbar}\langle[X^\alpha(\mathbf{q}), X^\beta(-\mathbf{q})]\rangle \tag{1.4}$$

and the transport coefficients can be written in terms of the Kubo relaxation matrix

$$\Gamma^{\alpha\beta}(\mathbf{q},\omega)=\Phi(\delta\dot{X}^\alpha(\mathbf{q}),\delta\dot{X}^\beta(\mathbf{q});\mathbf{q},\omega) \tag{1.5}$$

of the nonconserved parts of the currents

$$\delta\dot{X}^\alpha(\mathbf{q})=\dot{X}^\alpha(\mathbf{q})+iC^{\alpha\beta}(\mathbf{q})\,X^\beta(\mathbf{q}). \tag{1.6}$$

The standard procedure of mode coupling theory consists in two steps [5]: *(i)* One considers only two-mode decay processes, which amounts to a factorisation of the Kubo formulas (1.5) after insertion of the equations of motion. *(ii)* One makes a Lorentzian approximation for the relaxation matrix. In principal one can solve directly the set of self-consistent equations for the shape functions resulting from step *(i)*. For the isotropic ferromagnet this was achieved by Hubbard [6] in the paramagnetic phase. For most practical purposes an excellent approximation for the linewidth can be obtained from the mode coupling equations including the second approximation.

2. Isotropic ferromagnets

In this chapter we study the critical dynamics of an isotropic ferromagnet, where the spins are coupled only by the short range isotropic exchange interaction. The resulting mode coupling equations for such a system have been known for a long time [7]. But only above T_c these equations have been solved numerically [1].

The Hamiltonian for such a spin system is given by

$$H=\int\frac{\mathrm{d}^3q}{(2\pi)^3}\left[(J_0+Jq^2)\,\delta^{ij}\right]S^i(\mathbf{q})\,S^j(-\mathbf{q}), \tag{2.1}$$

where $S^i(\mathbf{q})$ are the Fourier transforms of the cartesian components $S^i(\mathbf{x})$ of the spin operator

$$S^i(\mathbf{q})=\int\mathrm{d}^3x\,\mathrm{e}^{\mathrm{i}\mathbf{q}\mathbf{x}}S^i(\mathbf{x}).$$

The coefficient J_0 does not enter the equations of motion explicitly and J denotes the strength of the exchange interaction. It is convenient to use the operators

$$S^\pm(\mathbf{q})=S^x(\mathbf{q})\pm iS^y(\mathbf{q}) \tag{2.2}$$

and $S^z(\mathbf{q})$ instead of the cartesian components of the spin operator. Then using the commutation relation for spin operators one finds the following set of equations of motion

$$\frac{\mathrm{d}}{\mathrm{d}t}S^z(\mathbf{q})=-iJ\int\frac{\mathrm{d}^3k}{(2\pi)^3}(2\mathbf{k}\mathbf{q}-q^2)\,S^+(\mathbf{q}-\mathbf{k})\,S^-(\mathbf{k}) \tag{2.3a}$$

$$\frac{\mathrm{d}}{\mathrm{d}t}S^\pm(\mathbf{q})=\pm i2J\int\frac{\mathrm{d}^3k}{(2\pi)^3}(2\mathbf{k}\mathbf{q}-q^2)\,S^\pm(\mathbf{q}-\mathbf{k})\,S^z(\mathbf{k}). \tag{2.3b}$$

2.1. Review of the mode coupling theory below the Curie temperature

In this section we review the derivation of the mode coupling equations for the isotropic ferromagnet below the Curie point, which was given already by one of the authors in a previous work [7].

Assuming that the spontaneous magnetization points along the z-axis the frequency matrix is given by

$$C^{\alpha\beta}(q)=\omega(q)\begin{bmatrix}0 & 0 & 0\\ 0 & +1 & 0\\ 0 & 0 & -1\end{bmatrix}, \tag{2.4a}$$

where $\alpha, \beta = z, +, -$. The frequency of the transverse modes is

$$\omega(q)=m/\chi^T(q), \tag{2.4b}$$

where $m=\langle S^z(q=0)\rangle$ denotes the magnetization and $\chi^T(q)$ the static transverse susceptibility. Due to the rotational symmetry of the Hamiltonian the Kubo relaxation matrix $\Phi^{\alpha\beta}(q,\omega)$ is diagonal

$$\Phi^{zz}(q,\omega)=\frac{i\chi^L(q)}{\omega+i\Gamma^{zz}(q,\omega)} \tag{2.5a}$$

$$\Phi^{\pm\pm}(q,\omega)=\frac{i\chi^{\pm}(q)}{\omega\mp\omega(q)+i\Gamma^{\pm\pm}(q,\omega)}, \tag{2.5b}$$

where $\chi^L(q)$ is the longitudinal susceptibility and $\chi^{\pm}(q)$ are related to the transverse susceptibility $\chi^+(q)=\chi^-(q)=2\chi^T(q)$.

Next we write down the Kubo formulas for the transport coefficients $\Gamma^{\alpha\alpha}(q,t)$; i.e.:

$$\Gamma^{zz}(q,t)=\frac{1}{\chi^L(q)}\Phi(\dot S_q^z(t),\dot S_q^z(0);q,t)\equiv\Gamma(q,t) \tag{2.6a}$$

$$\Gamma^{\pm\pm}(q,t)$$
$$=\frac{1}{2\chi^T(q)}\Phi(\dot S_q^{\pm}(t)\pm i\omega(q)S_q^{\pm}(t),\dot S_q^{\pm}(0)\pm i\omega(q)S_q^{\pm}(0);q,t)$$
$$\equiv\Lambda^{\pm}(q,t) \tag{2.6b}$$

Then we insert the equations of motion into these transport coefficients and make a factorisation approximation, which gives the following set of integral equations [7]

$$\Gamma(q,\omega)=\frac{J^2}{\chi^L(q)}k_BT\int\frac{dv}{2\pi}\int\frac{d^3k}{(2\pi)^3}\cdot[2\mathbf{qk}-q^2]^2\,\Phi^{++}(|\mathbf{q}-\mathbf{k}|,\omega-v)\,\Phi^{--}(k,v) \tag{2.7a}$$

$$\Lambda^{\pm}(q,\omega)=2\frac{J^2}{\chi^T(q)}k_BT\int\frac{dv}{2\pi}\int\frac{d^3k}{(2\pi)^3}\cdot[2\mathbf{qk}-q^2]^2\,\Phi^{\pm\pm}(|\mathbf{q}-\mathbf{k}|,\omega-v)\,\Phi^{zz}(k,v). \tag{2.7b}$$

Equations (2.7a, b) together with (2.5) constitute a complete set of self-consistent integral equations for the Kubo relaxation functions $\Phi^{\alpha\alpha}(q,\omega)$, which in principal could be solved numerically. For $m=0$ and $\chi^L=\chi^T$ (2.7a, b) reduce to the mode coupling equations for the paramagnetic phase, which were solved by Hubbard [6]. In the ferromagnetic phase (2.7a, b) have been solved in limiting cases [7]. Here we proceed by making the additional approximation that the relaxation functions are Lorentzians

$$\Phi^{zz}(q,\omega)=\frac{i\chi^L(q)}{\omega+i\Gamma(q)} \tag{2.8a}$$

$$\Phi^{\pm\pm}(q,\omega)=\frac{2i\chi^T(q)}{\omega\mp\omega(q)+i\Lambda^{\pm}(q)} \tag{2.8b}$$

with

$$\Gamma(q)=\Gamma(q,0)\text{ and }\Lambda(q)=\Lambda^+(q)=\Lambda^-(q)^*=\Lambda^+(q,\omega(q)).$$

The frequency integrals can now be carried out readily and one finds the following set of coupled integral equations for the linewidths

$$\Gamma(q)=iJ^2k_BT\int\frac{d^3k}{2\pi^3}\frac{\chi^T(|\mathbf{q}-\mathbf{k}|)\,\chi^T(k)}{\chi^L(q)}\cdot\frac{[2\mathbf{qk}-q^2]^2}{-\omega(|\mathbf{q}-\mathbf{k}|)+\omega(k)+i\Lambda(|\mathbf{q}-\mathbf{k}|)+i\Lambda^*(k)} \tag{2.9a}$$

$$\Lambda(q)=iJ^2k_BT\int\frac{d^3k}{2\pi^3}\frac{\chi^T(|\mathbf{q}-\mathbf{k}|)\,\chi^L(k)}{\chi^T(q)}\cdot\frac{[2\mathbf{qk}-q^2]^2}{\omega(q)-\omega(k)+i\Lambda(|\mathbf{q}-\mathbf{k}|)+i\Gamma(k)}. \tag{2.9b}$$

As is easily seen $\Gamma(q)$ is real, but $\Lambda(q)$ in general is complex. The imaginary part of the transverse damping function $\Lambda(q)$ leads to a shift of the frequency of the transverse spin waves, which however is a negligible correction with respect to the frequency matrix (2.4) as will be seen later. In the hydrodynamic regime (2.9a, b) can be solved analytically with the result

$$\Gamma(q)\propto\frac{q}{\chi^L(q)}\quad\text{and}\quad\Lambda(q)\propto q^4(c_1\ln(1/q\xi)+c_0), \tag{2.10}$$

where c_0 and c_1 are constants.

With the well known scaling properties of the static susceptibilities neglecting the Fisher exponent η

$$\chi^{L,T}(q)=J^{-1}q^{-2}\hat\chi^{L,T}(x) \tag{2.11}$$

(2.4b) gives

$$\omega(q)=A q^z \hat{\omega}(x) \tag{2.12a}$$

where the dynamical critical exponent z equals 5/2 and the scaling variable x is given by $x=1/q\xi$.

The scaling function for the bare frequency of the transverse modes can be written as

$$\hat{\omega}(x)=\begin{cases}\pi^{3/2}x^{1/2} & \text{for } T\leqq T_c\\ 0 & \text{for } T\geqq T_c.\end{cases} \tag{2.12b}$$

Hence (2.9a, b) can be solved by

$$\Gamma(q)=A q^z \gamma(x), \qquad \Lambda(q)=A q^z \lambda(x), \tag{2.13}$$

where the dynamical scaling functions γ and λ obey the following set of coupled integral equations

$$\gamma(x)=(2\pi)^2 i \int_{-1}^{+1} d\eta \int_0^\infty d\rho\, \rho_-^{-2}(\rho\eta-\tfrac{1}{2})^2 \frac{\hat{\chi}^T\left(\frac{x}{\rho_-}\right)\hat{\chi}^T\left(\frac{x}{\rho}\right)}{\hat{\chi}^L(x)} \cdot \frac{1}{-\rho^z\hat{\omega}(x/\rho)+\rho_-^z\hat{\omega}(x/\rho_-)+i\rho^z\lambda(x/\rho)+i\rho_-^z\lambda^*(x/\rho_-)} \tag{2.14a}$$

and

$$\lambda(x)=(2\pi)^2 i \int_{-1}^{+1} d\eta \int_0^\infty d\rho\, \rho_-^{-2}(\rho\eta-\tfrac{1}{2})^2 \frac{\hat{\chi}^L\left(\frac{x}{\rho_-}\right)\hat{\chi}^T\left(\frac{x}{s}\right)}{\hat{\chi}^T(x)} \cdot \frac{1}{\hat{\omega}(x)-\rho_-^z\hat{\omega}(x/\rho_-)+i\rho^z\lambda(x/\rho)+i\rho_-^z\gamma(x/\rho_-)}. \tag{2.14b}$$

Here we have used the notation $\rho=k/q$, $\rho_-=|\mathbf{q}-\mathbf{k}|/q$, $\eta=\cos(\mathbf{k},\mathbf{q})$ and the nonuniversal prefactor A is found to be

$$A=a^{5/2}(J k_B T/4\pi^4)^{1/2}.$$

The static correlation functions are known from renormalization group calculations. Neglecting Fisher-Langer corrections the static correlation function in the paramagnetic phase is given by an Ornstein-Zernike expression

$$\hat{\chi}(x)=\frac{1}{1+x^2}. \tag{2.15}$$

For the ferromagnetic phase Mazenko [8] has computed the longitudinal static susceptibility to first order in $\varepsilon=4-d$ using Wilson's matching technique

$$\chi^L(q)^{-1}=Jq^2\left[1-\frac{9\varepsilon}{n+8}x^2\left\{1+(1+4x^2)^{1/2}\cdot\ln\left[\frac{(1+4x^2)^{1/2}-1}{2x}\right]\right\}+x^2\left\{\frac{n+8+(5-n/2)\varepsilon}{9+(n-1)x^\varepsilon}\right\}\right], \tag{2.16a}$$

where n is the number of spin components. The last term in χ^L results from the presence of Goldstone modes below T_c. To the same order the transverse correlation function is given by

$$\chi^T(q)=J^{-1}/q^2. \tag{2.16b}$$

2.2 *Numerical solution of the mode coupling equations below T_c*

Introducing the static susceptibility (2.16a, b) we have solved the set of coupled integral Eq. (2.14a, b) by a self-consistent numerical procedure. The results are shown in Fig. 1a and b.

One recognizes that the scaling function Im $\lambda(x)$ for the frequency shift of the transverse modes is very small compared to $\hat{\omega}(x)$. In the critical region Im $\lambda(x)$ starts at the critical point with infinite slope and is negative in the hydrodynamical region. The scaling functions for the longitudinal and transverse linewidths split off linearly at the critical temperature and differ by orders of magnitude in the hydrodynamic region. This linear split-off of the longitudinal and transverse widths and the infinite slope of the frequency shift at the critical temperature below T_c is an immediate consequence of the presence of Goldstone modes. This can be derived analytically from (2.14). Namely, by differentiating (2.14a, b) with respect to x and setting $x=0$, we find

$$\left.\frac{\partial\gamma(x)}{\partial x}\right|_{x=0}=a_1+a_2\left.\frac{\partial\,\mathrm{Re}\,\lambda(x)}{\partial x}\right|_{x=0}$$

$$\left.\frac{\partial\,\mathrm{Re}\,\lambda(x)}{\partial x}\right|_{x=0}=a_3+a_4\left.\frac{\partial\,\mathrm{Re}\,\lambda(x)}{\partial x}\right|_{x=0}+a_5\left.\frac{\partial\gamma(x)}{\partial x}\right|_{x=0}$$

$$\left.\frac{\partial\,\mathrm{Im}\,\lambda(x)}{\partial x}\right|_{x\ll 1}=a_6 x^{-1/2}$$

where a_i are constants.

Above T_c the scaling function for the linewidth starts quadratically, as can be seen from

$$\left.\frac{\partial\gamma(x)}{\partial x}\right|_{x=0}\cdot\left[1+\frac{(2\pi)^2}{\gamma^2(0)}\int d\eta\int d\rho\,\rho_-^{-2}(\rho\eta-\tfrac{1}{2})^2\frac{\rho^{z-1}+\rho_-^{z-1}}{\rho_-^z+\rho^z}\right]=0,$$

which implies $\left.\frac{\partial\gamma(x)}{\partial x}\right|_{x=0}=0$. This analytic mode coupling result above T_c is in agreement with a renormalization group calculation by Iro [9], but is in contrast to the numerically found infinite slope of Hubbard [6]. It disagrees also with a computation of Ferrell

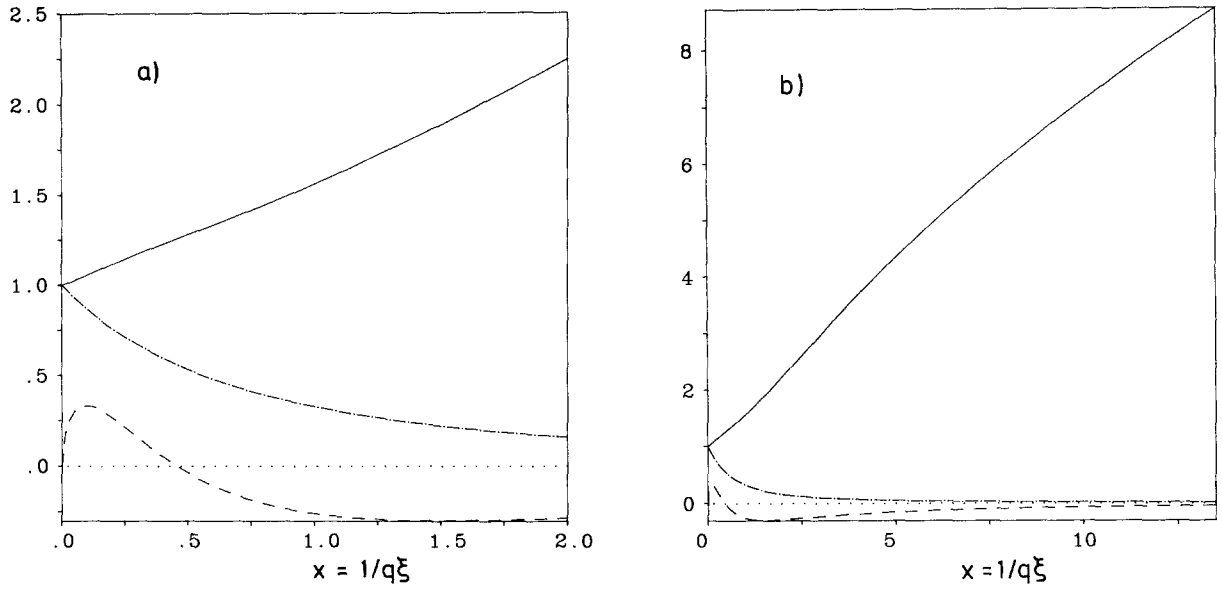

Fig. 1. a Dynamical scaling functions for ferromagnets with short range exchange interaction only versus $x=1/q\xi$ below T_c; γ solid, Reλ point-dashed and 10*Im λ dashed. **b** The same as Fig. 1a on a larger scale including the hydrodynamic region

and Bhattacharjee [10], who find, using Ward identities, a linear dependence on $1/q\xi$.

The numerical data can be fitted in the limits $x \gg 1$ (hydrodynamical region) and $x \ll 1$ (critical region) by simple functions as summarized in Table 1 (note that all functions are given in units of the value at criticality $\gamma(0)=\mathrm{Re}\,\lambda(0)=5.1326$)

The critical dynamics below the transition temperature has been studied also by renormalization group methods. Ma and Mazenko [11] calculated the transport coefficient for the longitudinal magnetization for small wave vectors in an ε-expansion ($\varepsilon=d-6$). Their result was

$$\Gamma(q)=\frac{\hat{\Gamma}(q)}{\chi_L(q)}q^2 \tag{2.17}$$

with

$$\hat{\Gamma}(q)\propto q^{(d-6)/6}. \tag{2.18}$$

With $\chi^L(q)\propto 1/q$ in $d=3$ dimensions this would give $\Gamma(q)\propto q^{5/2}$ in contradiction to the mode coupling result for small q (i.e. in the hydrodynamical limit [7]). However, Sasvári's [12] reanalysis of Ma and Mazenko's exponentiation method showed, that taking into account the regular parts of $\hat{\Gamma}(q)$ results in

$$\hat{\Gamma}(q)=q^{(d-6)/3}. \tag{2.19}$$

This leads to $\Gamma(q)\propto q^2$ for $d=3$, in agreement with the mode coupling result in Table 1. The q^4-dependence of the transverse transport coefficient in the hydrodynamical limit is also confirmed by the renormalization group calculations [11].

Experimental investigations of the critical dynamics below T_c have been performed by means of unpolarized neutron scattering by Collins et al. [13] on iron, by Minkiewicz et al. [14] on Ni and by Dietrich et al. [15] on EuO. However, only the side-peaks originating from the transverse spin waves have been observed, without any evidence for the central peak due to the longitudinal spin diffusion. This is plausible in the light of the mode coupling results. In the hydrodynamical region ($x=1/q\xi \gg 1$) the width of the longitudinal peak is much wider than the separation of the transverse peaks [7]. Moreover, its intensity is smaller than that of the transverse magnons, which

Table 1. Asymptotic behaviour of the scaling functions below the critical temperature in units of the value at criticality $\gamma(0)$

	$\gamma(x)/\gamma(0)$	$\Gamma(q)$	$\mathrm{Re}\,\lambda(x)/\gamma(0)$	$\mathrm{Im}\,\lambda(x)/\gamma(0)$	$\mathrm{Im}\,\Lambda(q)$ / $\mathrm{Re}\,\Lambda(q)$
$x\gg 1$	$1.37+0.37\dfrac{x^{-1/2}}{\hat{\chi}_L(x)}$	$q^2\xi^{-1/2}$	$0.16x^{-1.5}\ln x$	$-0.07x^{-1.5}\ln x$	$q^4\xi^{3/2}\ln\left(\dfrac{1}{q\xi}\right)$
$x\ll 1$	$1.0+0.55x$	$q^{5/2}$	$1.0-1.34x$	$0.77x^{1/2}$	$q^2\xi^{-1/2}; q^{5/2}$

altogether implies that it may be very difficult to distinguish the longitudinal peak from the background. In the critical region the linewidths are of the same order of magnitude. In this limit however the frequency of the transverse modes tends to zero. Using unpolarized neutrons one can only observe a superposition of the peaks. Lacking a theory for the linewidth in the critical region below T_c it was impossible up to now to resolve the longitudinal and transverse peaks.

A first observation of the longitudinal peak was reported recently by Mitchell et al. [16] using polarized neutrons. However, there are not enough data to compare with the theoretical predictions, also, the material is disordered (palladium with 10% iron).

In Fig. 2 we show $S^{xx}(q,\omega)=S^{yy}(q,\omega)$ and $S^{zz}(q,\omega)$ for parameters corresponding to EuO for a series of temperatures close to the Curie point ($(T_c-T)/T_c=0.150$, 0.075, 0.050, 0.020, 0.005), where the wave vector is fixed to $q=0.2$ Å^{-1}. In the presence of domains, such that the magnetization points with equal propability along the x, y and z-directions, one measures in neutron scattering experiments

$$S_{av}(q,\omega)=\tfrac{1}{3}(2S^{xx}(q,\omega)+S^{zz}(q,\omega)),$$

which is also shown in Fig. 2.

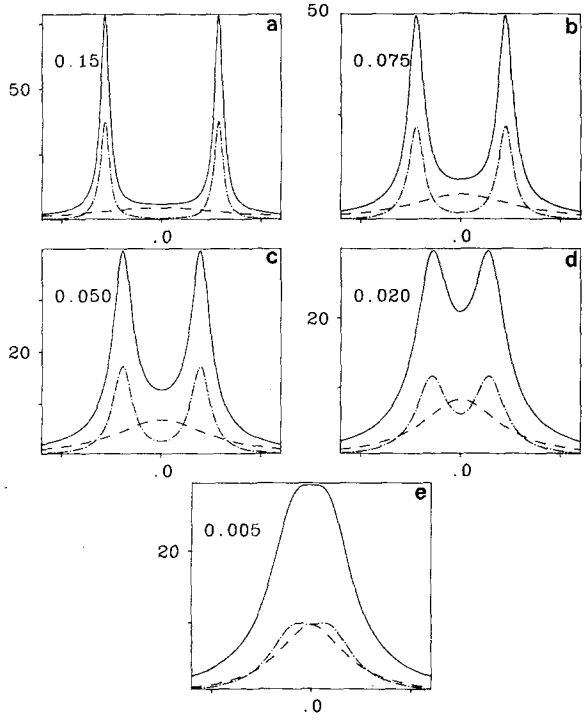

Fig. 2 a–e. Dynamic structure functions $S^{xx}(q,\omega)=S^{yy}(q,\omega)$ (point-dashed), $S^{zz}(q,\omega)$ (dashed) and $3\cdot S_{av}(q,\omega)$ (solid) for EuO at the wave vector $q=0.2$ Å^{-1}. The reduced temperatures $(T_c-T)/T_c$ are: **a** 0.150, **b** 0.075, **c** 0.050, **d** 0.020, **e** 0.005

The qualitative similarity of $S_{av}(q,\omega)$ to Fig. 4 of [15] is striking. For a quantitative comparison the theory has to be convoluted with the instrumental resolution function. In addition $S_{av}(q,\omega)$ has to be multiplied by the detailed balance factor $\frac{\beta\omega}{1-e^{-\beta\omega}}$. And most important, close to T_c dipolar effects not contained in our theory for the ordered phase will be significant, as can be inferred from our analysis of the paramagnetic phase described in the next section.

3. Dipolar ferromagnets

Above T_c the critical dynamics of isotropic ferromagnets such as EuO, EuS and Fe has been studied by various experimental methods, sampling different regions in q-space. These measurements indicate that the critical dynamics of isotropic ferromagnets cannot be explained solely on the basis of the short range exchange interaction. There were however apparent discrepancies for the following reasons.

Hyperfine interaction experiments and electron spin resonance experiments show a distinct crossover in the dynamical exponent from the isotropic $z=5/2$ to the dipolar $z=2$ as a function of the temperature [17–22]. On the other hand the critical exponent deduced from the wavevector dependence of the neutron scattering data right at the critical temperature is 5/2 [23–26]. But nevertheless the data could not be fitted by the Resibois-Piette [1] scaling function for isotropic ferromagnets [23]. Those apparent discrepancies remained a puzzle up to now and prompted a variety of interpretations including suggestions that dipolar forces might not be relevant for the dynamics of these magnets and that the data showed signatures of randomness and additional relaxation mechanisms.

It is the aim of this chapter to show that all these experiments can be explained on the basis of the mode coupling theory in a unifying fashion taking into account the dipolar interaction, which is present in all real ferromagnets.

3.1 Mode coupling equations for dipolar ferromagnets

In this section we evaluate the dynamical scaling functions for weak dipolar ferromagnets in the paramagnetic phase. Part of the results have been already reported recently [3]. Here we present further details and extend the theory to ESR and NMR.

The Hamiltonian for a spin system with both short range exchange and long range dipolar interac-

tions is given by

$$H=\int\frac{\mathrm{d}^3q}{(2\pi)^3}\left[(J_0+Jq^2)\,\delta^{ij}+Jg\frac{q^iq^j}{q^2}\right]S^i(\mathbf{q})\,S^j(-\mathbf{q}), \tag{3.1}$$

where we have used the same notation as in Sect. 2. The parameter

$$g=a_1(g_L\mu_B)^2/2Ja^3 \tag{3.2}$$

characterises the ratio of dipolar to exchange interactions. Here g_L is the Landé factor and the coefficient a_1 depends on the lattice structure; i.e.: $a_1=4\pi$(sc), $3^{3/2}\pi$(bcc), $2^{5/2}\pi$(fcc). In (3.1) we assumed that the dipolar forces are weaker than the exchange interaction [2]; i.e. $g\ll 1$.

Due to the symmetry of the Hamiltonian it is necessary to decompose the spin operators $\mathbf{S}(\mathbf{q})$ into a longitudinal and two transverse components with respect to the wavevector $\mathbf{q}$

$$\mathbf{S}(\mathbf{q})=S^L(\mathbf{q})\,\hat{q}+S^{T_1}(\mathbf{q})\,\hat{t}^1(\hat{q})+S^{T_2}(\mathbf{q})\,\hat{t}^2(\hat{q}), \tag{3.3}$$

where the orthonormal set of unit vectors is defined by

$$\hat{q}=\mathbf{q}/q,\qquad \hat{t}^1(\hat{q})=\mathbf{q}\times\mathbf{e}_3/(q_1^2+q_2^2)^{1/2}$$

and

$$\hat{t}^2(\hat{q})=\hat{q}\times\hat{t}^1(\hat{q}).$$

For vanishing components of $\mathbf{q}$ the limits are taken in the order of increasing cartesian components. The Heisenberg equations of motion are found to be

$$\begin{aligned}\dot{S}^L_{\mathbf{q}}=&J\int\frac{\mathrm{d}^3k}{(2\pi)^3}\frac{1}{k}\\&\cdot[\mathbf{q}(2\mathbf{k}-\mathbf{q})[(k_1^2+k_2^2)^{1/2}\{S^{T_1}_{\mathbf{q}-\mathbf{k}},S^L_{\mathbf{k}}\}+k_3\{S^{T_1}_{\mathbf{q}-\mathbf{k}},S^{T_2}_{\mathbf{k}}\}]\\&+g(k_1^2+k_2^2)^{1/2}\{S^{T_1}_{\mathbf{q}-\mathbf{k}},S^L_{\mathbf{k}}\}]\end{aligned} \tag{3.4a}$$

$$\begin{aligned}\dot{S}^{T_1}_{\mathbf{q}}=&-J\int\frac{\mathrm{d}^3k}{(2\pi)^3}\frac{1}{k}\\&\cdot\left[\mathbf{q}(2\mathbf{k}-\mathbf{q})\left[\frac{-k_1k_3}{(k_1^2+k_2^2)^{1/2}}\{S^{T_1}_{\mathbf{q}-\mathbf{k}},S^L_{\mathbf{k}}\}+k_1\{S^{T_1}_{\mathbf{q}-\mathbf{k}},S^{T_2}_{\mathbf{k}}\}\right.\right.\\&+\frac{k_2(k_3q-k^2)}{|\mathbf{q}-\mathbf{k}|\,(k_1^2+k_2^2)^{1/2}}\{S^{T_2}_{\mathbf{q}-\mathbf{k}},S^L_{\mathbf{k}}\}+\frac{1}{2}\frac{k_2q}{|\mathbf{q}-\mathbf{k}|}\{S^L_{\mathbf{q}-\mathbf{k}},S^L_{\mathbf{k}}\}\\&\left.-\frac{1}{2}\frac{k_2q}{|\mathbf{q}-\mathbf{k}|}\{S^{T_2}_{\mathbf{q}-\mathbf{k}},S^{T_2}_{\mathbf{k}}\}\right]\\&+g\left[\frac{-k_1k_3}{(k_1^2+k_2^2)^{1/2}}\{S^{T_1}_{\mathbf{q}-\mathbf{k}},S^L_{\mathbf{k}}\}\right.\\&\left.\left.+\frac{k_2(k_3q-k^2)}{|\mathbf{q}-\mathbf{k}|\,(k_1^2+k_2^2)^{1/2}}\{S^{T_2}_{\mathbf{q}-\mathbf{k}},S^L_{\mathbf{k}}\}\right]\right]\end{aligned} \tag{3.4b}$$

and for $S^{T_2}_{\mathbf{q}}$ correspondingly, where $\{,\}$ denotes the anit-commutator. The terms proportional to g, resulting from the dipolar term in the Hamiltonian remain finite as the wave vector q tends to zero, whereas all the other terms vanish in this limit. This reflects the fact that the dipolar forces lead to a relaxational dynamic in the limit of long wavelengths.

Now we start with the first step of the mode coupling theory and make, after insertion of the equations of motion (3.4a, b) into the transport coefficients

$$\Gamma^L(q,g,t)=\frac{1}{\chi^L(q)}\,\Phi(\dot{S}^L(\mathbf{q},t),\dot{S}^L(\mathbf{q},0);q,g,t)$$

$$\begin{aligned}\Gamma^T(q,g,t)&=\frac{1}{\chi^T(q)}\,\Phi(\dot{S}^{T_1}(\mathbf{q},t),\dot{S}^{T_1}(\mathbf{q},0);q,g,t)\\&=\frac{1}{\chi^T(q)}\,\Phi(\dot{S}^{T_2}(\mathbf{q},t),\dot{S}^{T_2}(\mathbf{q},0);q,g,t),\end{aligned}$$

the factorisation approximation. This leads to

$$\begin{aligned}\Gamma^L(q,g,t)=&\frac{4J^2k_BT}{\chi^L(q)}\int\frac{\mathrm{d}^3k}{(2\pi)^3}\\&\cdot[v^L_{TT}(k,q,g,\Theta)\,\Phi^T(k,g,t)\,\Phi^T(|\mathbf{q}-\mathbf{k}|,g,t)\\&+v^L_{LT}(k,q,g,\Theta)\,\Phi^L(k,g,t)\,\Phi^T(|\mathbf{q}-\mathbf{k}|,g,t)]\end{aligned} \tag{3.5a}$$

$$\begin{aligned}\Gamma^T(q,g,t)=&\frac{4J^2k_BT}{\chi^T(q)}\int\frac{\mathrm{d}^3k}{(2\pi)^3}\\&\cdot[v^T_{TT}(k,q,g,\Theta)\,\Phi^T(k,g,t)\,\Phi^T(|\mathbf{q}-\mathbf{k}|,g,t)\\&+v^T_{LT}(k,q,g,\Theta)\,\Phi^L(k,g,t)\,\Phi^T(|\mathbf{q}-\mathbf{k}|,g,t)\\&+v^T_{LL}(k,q,g,\Theta)\,\Phi^L(k,g,t)\,\Phi^L(|\mathbf{q}-\mathbf{k}|,g,t)],\end{aligned} \tag{3.5b}$$

where the vertex functions $v^\alpha_{\beta\sigma}$ for the decay of the mode α into the modes β and σ are given by

$$v^L_{TT}(k,q,g,\eta)=2\cos^2\Theta\,q^4\left(\frac{k\cos\Theta}{q}-0.5\right)^2 \tag{3.6a}$$

$$v^L_{LT}(k,q,g,\eta)=2\sin^2\Theta\,q^4\left(\frac{k\cos\Theta}{q}-0.5+\frac{g}{2q^2}\right)^2 \tag{3.6b}$$

$$\begin{aligned}v^T_{TT}(k,q,g,\eta)=&q^4\sin^2\Theta\left(1+\frac{q^2}{2|\mathbf{q}-\mathbf{k}|^2}\right)\\&\cdot\left(\frac{k\cos\Theta}{q}-0.5\right)^2\end{aligned} \tag{3.6c}$$

$$\begin{aligned}v^T_{LT}(k,q,g,\eta)=&q^4\left[2-\left(1+\frac{q^2}{|\mathbf{q}-\mathbf{k}|^2}\right)\sin^2\Theta\right]\\&\cdot\left(\frac{k\cos\Theta}{q}-0.5+\frac{g}{2q^2}\right)^2\end{aligned} \tag{3.6d}$$

$$v^T_{LL}(k,q,g,\eta)=\sin^2\Theta\,q^4\frac{q^2}{2|\mathbf{q}-\mathbf{k}|^2}\left(\frac{k\cos\Theta}{q}-0.5\right)^2 \tag{3.6e}$$

where $\eta=\cos\Theta$.

In an attempt to derive mode coupling equations for dipolar ferromagnets Borckmans et al. [27] used a decomposition of the spin operator (see (3.3)) with one perpendicular direction $\mathbf{u}(\mathbf{q})$ only, which then is time dependent. Lacking an equation of motion for $\mathbf{u}(\mathbf{q})$, the vertices in the mode coupling equations necessary for the computation of the scaling functions could not be determined.

The mode coupling result for the transport coefficients (3.5a, b) together with the expressions

$$\Phi^L(q,g,\omega)=i\frac{\chi^L(q,g)}{\omega+i\Gamma^L(q,g,\omega)} \tag{3.7a}$$

$$\Phi^T(q,g,\omega)=i\frac{\chi^T(q,g)}{\omega+i\Gamma^T(q,g,\omega)} \tag{3.7b}$$

for the Kubo relaxation functions constitute, as in Sect. 2, a complete set of self-consistent equations, which could in principal be solved numerically. If the transport coefficients vary only slowly with ω we may approximate our relaxation functions by Lorentzians; i.e. we replace the transport coefficients in (3.7a, b) by their values at $\omega=0$:

$$\Gamma^L(q,g)=\Gamma^L(q,g,\omega=0) \quad \text{and} \quad \Gamma^T(q,g)=\Gamma^T(q,g,\omega=0).$$

This additional approximation finally leads to the following set of coupled integral equations for the transverse and longitudinal linewidth above the transition temperature

$$\Gamma^L(q,g)=\frac{J^2 k_B T}{\pi^2\chi^L(q,g)}\int_{-1}^{+1}\mathrm{d}\eta\int_0^\infty \mathrm{d}k k^2 \cdot\left[v_{TT}^L(k,q,g,\eta)\frac{\chi^T(k,g)\,\chi^T(|\mathbf{q}-\mathbf{k}|,g)}{\Gamma^T(k,g)+\Gamma^T(|\mathbf{q}-\mathbf{k}|,g)} +v_{LT}^L(k,q,g,\eta)\frac{\chi^L(k,g)\,\chi^T(|\mathbf{q}-\mathbf{k}|,g)}{\Gamma^L(k,g)+\Gamma^T(|\mathbf{q}-\mathbf{k}|,g)}\right] \tag{3.8a}$$

$$\Gamma^T(q,g)=\frac{J^2 k_B T}{\pi^2\chi^T(q,g)}\int_{-1}^{+1}\mathrm{d}\eta\int_0^\infty \mathrm{d}k k^2 \cdot\left[v_{TT}^T(k,q,g,\eta)\frac{\chi^T(k,g)\,\chi^T(|\mathbf{q}-\mathbf{k}|,g)}{\Gamma^T(k,g)+\Gamma^T(|\mathbf{q}-\mathbf{k}|,g)} +v_{LT}^T(k,q,g,\eta)\frac{\chi^L(k,g)\,\chi^T(|\mathbf{q}-\mathbf{k}|,g)}{\Gamma^L(k,g)+\Gamma^T(|\mathbf{q}-\mathbf{k}|,g)} +v_{LL}^T(k,q,g,\eta)\frac{\chi^L(k,g)\,\chi^L(|\mathbf{q}-\mathbf{k}|,g)}{\Gamma^L(k,g)+\Gamma^L(|\mathbf{q}-\mathbf{k}|,g)}\right]. \tag{3.8b}$$

The essential point now is that the mode coupling (3.8) are consistent with the generalised dynamical scaling law

$$\Gamma^\alpha(q,g)=\Lambda q^z\gamma^\alpha(x,y), \tag{3.9}$$

where in the present case we have to introduce the two scaling variables

$$x=1/q\xi \quad \text{and} \quad y=g^{1/2}/q \tag{3.10}$$

and $z=5/2$. The crossover of the critical dynamical exponent z is contained in the scaling functions $\gamma^\alpha(x,y)$. Two parameter scaling laws have been introduced by Riedel and Wegner [28] for anisotropic magnets. Introducing (3.9) and (3.10) as well as

$$\chi^\alpha(q,g)=J^{-1}q^{-2}\hat{\chi}^\alpha(x,y) \tag{3.11}$$

into (3.8a, b), we find for the dynamical scaling functions

$$\gamma^\alpha(x,y)=\frac{2\pi^2}{\hat{\chi}^\alpha(x,y)}\int_{-1}^{1}\mathrm{d}\eta\int_0^\infty\mathrm{d}\rho\sum_\beta\sum_\sigma\hat{v}_{\beta\sigma}^\alpha(y,\rho,\eta) \cdot(\delta_{\sigma,T}+\delta_{\alpha,T}\delta_{\beta,L}\delta_{\sigma,L}) \cdot\frac{\rho_-^{-2}\hat{\chi}^\beta\left(\frac{x}{\rho},\frac{y}{\rho}\right)\hat{\chi}^\sigma\left(\frac{x}{\rho_-},\frac{y}{\rho_-}\right)}{\rho^{5/2}\gamma^\beta\left(\frac{x}{\rho},\frac{y}{\rho}\right)+\rho_-^{5/2}\gamma^\sigma\left(\frac{x}{\rho_-},\frac{y}{\rho_-}\right)} \tag{3.12}$$

and the nonuniversal frequency scale of (3.9)

$$\Lambda=a^{5/2}(Jk_B T/2\pi^4)^{1/2}=g_L\mu_B(k_B T a_1/4\pi^4)^{1/2}/q_D. \tag{3.13}$$

If Λ is expressed by $q_D=g^{1/2}/a$, the lattice structure dependence of a_1 has to be considered, which increases the theoretical Λ of Fe by a factor of 1.14 as compared to [24]. We note that this is the same nonuniversal frequency scale as for isotropic ferromagnets without dipolar interaction ($\Lambda=A$). In (3.12) we used the same notation as in Sect. 2 and introduced the scaled vertex functions

$$\hat{v}_{\beta\beta}^\alpha=\left[2\eta^2\delta_{\alpha,L}+(1-\eta^2)\left(\delta_{\beta,T}+\frac{1}{2\rho_-^2}\right)\delta_{\alpha,T}\right](\rho\eta-\tfrac{1}{2})^2 \tag{3.14a}$$

$$\hat{v}_{L,T}^\alpha=\left[2(1-\eta^2\delta_{\alpha,L})-(1-\eta^2)\left(1+\frac{1}{\rho_-^2}\right)\delta_{\alpha,T}\right] \cdot\left(\rho\eta-\frac{1}{2}+\frac{y^2}{2}\right)^2, \tag{3.14b}$$

which are related to $v_{\beta\sigma}^\alpha$ by

$$v_{\beta\sigma}^\alpha=q^4\hat{v}_{\beta\sigma}^\alpha.$$

For both longitudinal and transverse modes, the dipolar interaction enters only in vertices for decays into a longitudinal and a transverse mode. As summarized in Table 2 the mode coupling Eq. (3.12) can be solved analytically in the dipolar (D) and isotropic

Table 2. Asymptotic behaviour of the scaling functions in the paramagnetic phase

	γ^T	γ^L
DC	$y^{1/2}$	$y^{5/2}$
IC	1	1
DH	$y^{1/2}x^2$	$y^{5/2}$
IH	$x^{1/2}$	$x^{1/2}$

(I) critical (C) and hydrodynamic (H) limiting regions. These are defined by DC: $y \gg 1$, $x \ll 1$; IC: $y \ll 1$, $x \ll 1$; DH: $y \gg x$, $x \gg 1$; IH: $y \ll x$, $x \gg 1$.

Concerning the critical dynamical exponent one finds for the longitudinal linewidth a crossover from $z=2.5$ in the isotropic critical region to $z=0$ in the dipolar critical region, whereas for the transverse linewidth the crossover is from $z=2.5$ to $z=2$. The precise position of this crossover can only be determined numerically. As we shall see in the next section, the dynamic crossover for the transverse width is shifted with respect to the static crossover to a wavevector smaller by almost one order of magnitude, whereas the crossover for the longitudinal width occurs at the static crossover.

As for the pure isotropic ferromagnet, the mode coupling equations do not account for effects of the critical exponent η, which will be neglected in the following. In the numerical calculations we will use the Ornstein Zernike forms for the static susceptibilities

$$\chi^{\alpha}(q, g) = J^{-1}(q^2 + \xi^{-2} + \delta_{\alpha,L}\, g)^{-1} \tag{3.15}$$

where $\xi = \xi_0((T - T_c)/T_c)^{-\nu}$ is the correlation length. The static crossover is contained in ξ through the effective exponent $\nu = \gamma_{\text{eff}}/2$ [29].

For the numerical solution of the coupled integral Eq. (3.12) it is convenient to introduce polar coordinates

$$r = (x^2 + y^2)^{1/2} \quad \text{and} \quad \varphi = \arctg \frac{y}{x} \tag{3.16}$$

with x and y defined in (3.10). The transverse and longitudinal scaling functions γ^T and γ^L are exhibited in Fig. 3 and Fig. 4, where all results are given in units of the value at criticality $\gamma_0 \equiv \gamma^{L(T)}(0, 0) = 5.1326$. For $\varphi = 0$, corresponding to vanishing g, the scaling functions coincide with the Resibois-Piette scaling function. The cut at $\varphi = \pi/2$ corresponds to $T = T_c$ with r reducing to $g^{1/2}/q$. The physical content of the two parameter scaling surfaces is illustrated best by considering cuts for fixed g and various temperatures. This will be given below in conjunction with our predictions for neutron scattering experiments.

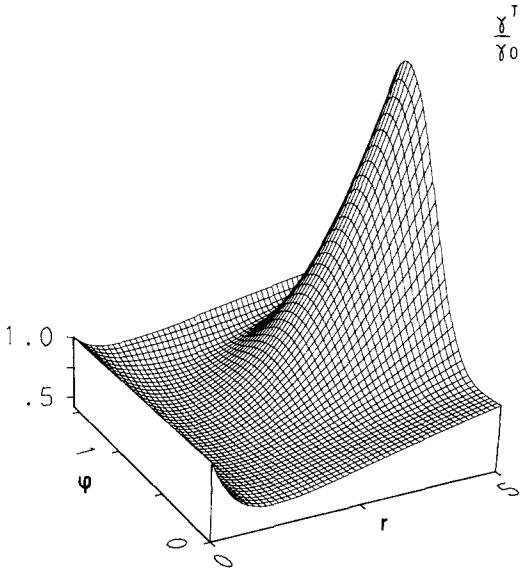

Fig. 3. Scaling function γ^T for the transverse width of dipolar ferromagnets above T_c versus $r = (q\xi)^{-1}(1 + g\xi^2)^{1/2}$ and $\varphi = \arctg(g^{1/2}\xi)$

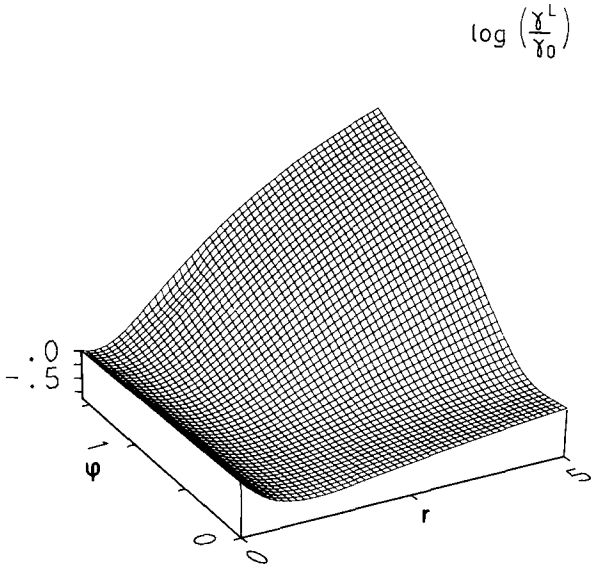

Fig. 4. Scaling function γ^L for the longitudinal width of dipolar ferromagnets above T_c versus r and φ defined in the caption to Fig. 3

3.2 Predictions for experiments

With the results of Sect. 3.1 we can now compare our theory with the various experimental results above the critical temperature. The most important experimental probes are neutron scattering, electron-spin resonance and hyperfine interaction experiments. With these methods one is able to investigate different regions in q-space. Hence all in all these experimental

studies give quite complete a picture of the critical dynamics.

3.2.1 Neutron scattering. In neutron scattering experiments one measures the cross-section for inelastic magnetic scattering. Therefore one is able to determine the dynamical scaling functions as functions of both temperature and wavevector.

In experimental studies it is convenient to plot the linewidth as a function of the single scaling variable $x=1/q\xi$. In Figs. 5 and Fig. 6 we display the scaling functions versus $x=1/q\xi$ for different values of $\varphi=\arctg\, g^{1/2}\xi=N\pi/40$ with $N=0, 1, \ldots, 19$. The curve $N=1$ is indistinguishable from the Resibois-Piette function, $N=0$. If g is finite, the curves approach the Resibois-Piette scaling function for small x and deviate therefrom with increasing x. For a given material, g is fixed and the parametrisation by φ corresponds to a parametrisation by $(T-T_c)$. The experimental results of Mezei on iron (Fig. 3 of [23] and Fig. 4 of [24]) taken at different temperatures show precisely the $(q\xi)^{-1}$ dependence exhibited by the transverse scaling function (Fig. 4). We are convinced that the uncertainty in the value of ξ_0, the improvement in the experimental analysis possible by taking into account the effective critical exponent [29] $\nu\cong\gamma_{\text{eff}}/2$ and the limits of the experimental accuracy, altogether leave enough room for a complete quantitative agreement with the theory.

To examine the dipolar crossover precisely at the Curie point, Fig. 7 displays the scaling functions for the transverse and longitudinal width for $T=T_c$ against the wave number; i.e.: $y^{-1}=q/g^{1/2}$. These results clearly show that the crossover from isotropic to dipolar critical dynamics in the transverse linewidth (Fig. 7) occurs at a wave number smaller than q_D, the position of the static crossover, by almost an order of magnitude. This purely dynamical shift of the crossover explains why, within the accessible wavevector region, this crossover escaped the detection by neutron scattering experiments. There is, however, an indication of an increase in the data for the transverse width at the smallest momentum transfer [30], as predicted by the theory.

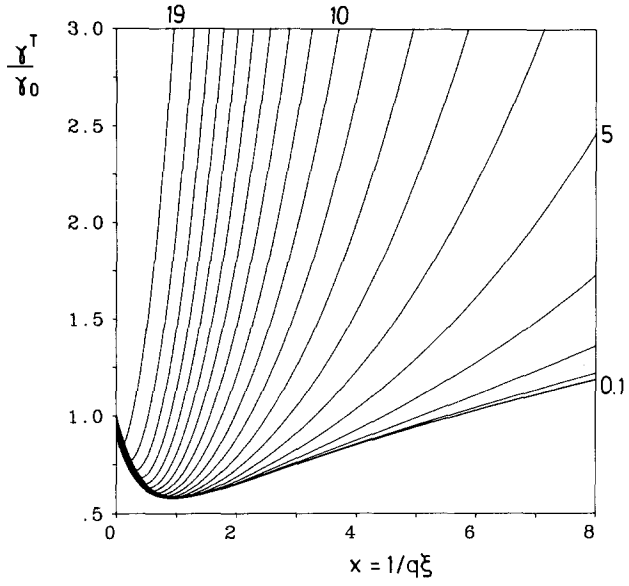

Fig. 5. Scaling function γ^T for the transverse width versus $(q\xi)^{-1}$ for values of $\varphi=N\pi/40$ with N indicated in the graph

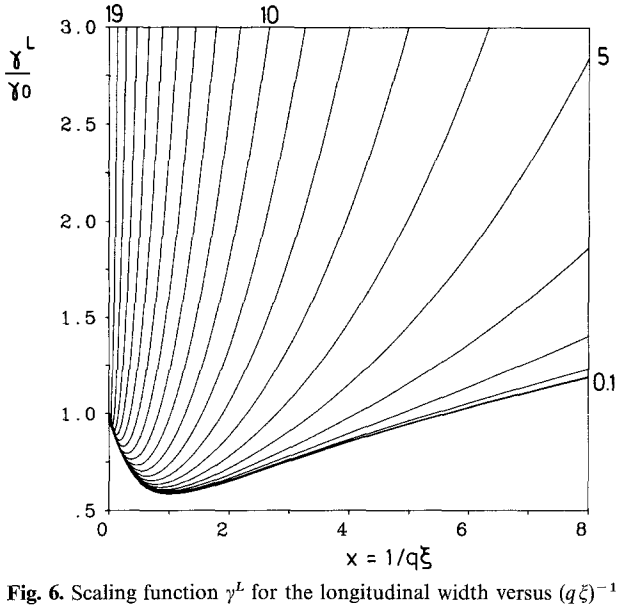

Fig. 6. Scaling function γ^L for the longitudinal width versus $(q\xi)^{-1}$ for values of $\varphi=N\pi/40$ with N indicated in the graph

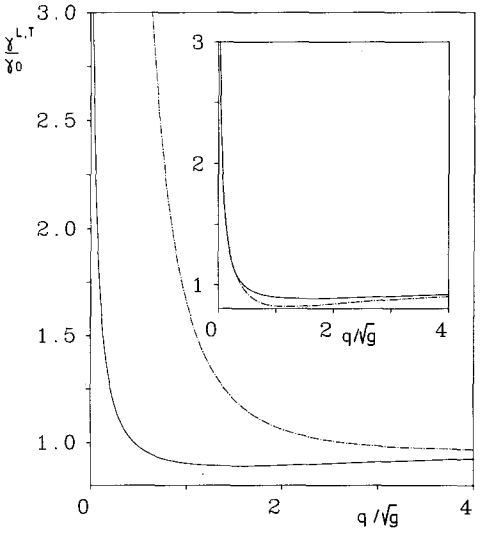

Fig. 7. Scaling functions for the longitudinal (point-dashed) and transverse (solid) widths vs. $qg^{-1/2}$ at the critical temperature. Inset: Scaling functions for the longitudinal (point-dashed) and transverse (solid) Onsager coefficients versus $qg^{-1/2}$ at the critical temperature

The crossover of the longitudinal width, from $z=2.5$ to $z=0$, is more pronounced and occurs in the immediate vicinity of q_D. It should be possible to test this prediction experimentally. The reason for the different location of the dynamic crossover is mainly due to the fact, that it is primarily the longitudinal static susceptibility which shows a crossover due to the dipolar interactions. Since the change in the static critical exponent is numerically small the transverse static susceptibility is nearly the same as for ferromagnets without dipolar interaction. Hence the crossover in the transverse width is purely a dynamical crossover, whereas the crossover of the longitudinal width being proportional to the inverse longitudinal susceptibility is enhanced by the static crossover. In order to exhibit these arguments we have plotted in the inset of Fig. 7 the scaling functions for the Onsager coefficients $\hat{\chi}^\alpha\gamma^\alpha$ at the critical temperature vs. $q/g^{1/2}$, showing only the dynamical crossover.

3.2.2 Electron spin resonance (ESR) experiments. In ESR-experiments one measures the electronic response function at zero wavevector and determines therefrom the Onsager coefficient. Turning to our mode coupling Eq. (3.8) we find that the longitudinal and transverse linewidths ($\alpha=L, T$) at zero wavevector are given by

$$\Gamma_0^\alpha(g)=\frac{4(gJ)^2}{3\pi^2\chi_0^\alpha(g)}k_BT\int_0^\infty \mathrm{d}k\,k^2 \cdot\frac{\chi^L(k,g)\,\chi^T(k,g)}{\Gamma^L(k,g)+\Gamma^T(k,g)}. \tag{3.17}$$

As before the temperature dependence of $\Gamma_0^\alpha(g)$ entering via ξ is not indicated explicitly. Introducing polar coordinates as in Sect. 3.1 and using the scaling properties of the static and dynamic quantities this coefficient can be written as

$$\Gamma_0^\alpha(g)=B\,F(g\xi^2)\,[\hat{\chi}_0^\alpha(g\xi^2)]^{-1}\equiv B\,\gamma_0(g\xi^2). \tag{3.18}$$

The universal crossover function F of the Onsager coefficient following from (3.17) is

$$F(g\xi^2)=\left(1+\frac{1}{g\xi^2}\right)^{-7/4}\int_0^\infty \mathrm{d}r\,r^{5/2} \cdot\frac{\hat{\chi}^L(r,\varphi)\,\hat{\chi}^T(r,\varphi)}{\gamma^L(r,\varphi)+\gamma^T(r,\varphi)} \tag{3.19}$$

and the scaling functions $\hat{\chi}_0^\alpha(g\xi^2)$ for the susceptibilities at zero wave vector are given by

$$\hat{\chi}_0^\alpha(g\xi^2)=\begin{cases}\dfrac{1}{1+(g\xi^2)^{-1}} & \text{for } \alpha=L\\ g\xi^2 & \text{for } \alpha=T.\end{cases} \tag{3.20}$$

Finally B denotes a nonuniversal constant

$$B=\frac{8\pi^2}{3}A\,q_D^{5/2}. \tag{3.21}$$

One has to be prepared for minor inaccuracies of constants as B, since the theory is not designed primarily for the determination of those nonuniversal constants.

Because the Onsager coefficient $\Gamma^\alpha\chi^\alpha$ does not depend on the sample shape [31] and is the same for the transverse and the longitudinal mode this quantity is the most convenient for a comparison with experiment. The universal function $F(g\xi^2)$ is plotted in Fig. 8. Its shape is dominated by the first factor in (3.19) whereas the integral is almost a constant leading to small corrections only. Therefore $F(q\xi^2)$ is mainly determined by the static crossover. In the strong dipolar limit (very close to the critical temperature) F approaches a constant in agreement with Finger's result [32] and in the crossover region we find a $\xi^{7/2}$ behavior in agreement with a mode coupling calculation of Raghaven and Huber [33]. If there were no dipolar interaction ($g=0$), one would simple find a vanishing Onsager coefficient due to the factor g^2 in (3.17). With regard to the crossover function F it is natural to define the reduced crossover temperature by

$$\tau_{\mathrm{cross}}=\frac{T_{\mathrm{cross}}-T_c}{T_c}=(g\xi_0^2)^{1/\Phi} \tag{3.22}$$

where the crossover exponent Φ equals the susceptibility exponent γ for a ferromagnet without dipolar interaction [2]. If one neglects the dipolar crossover in the correlation length, the scaling variable $g\xi^2$ can

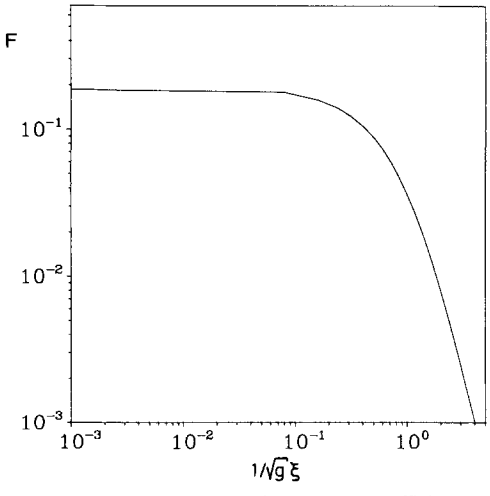

Fig. 8. Scaling function for the Onsager coefficient at zero wavevector versus $(g^{1/2}\xi)^{-1}$

be written as $g\xi^2=(\tau_{\text{cross}}/\tau)^{\gamma}$ and the crossover temperature in terms of the dipolar wavevector is given by

$$q_D\,\xi_{\text{cross}}=1. \tag{3.23}$$

The crossover temperatures resulting from (3.23) can be found in [24]. With this approximation and $\gamma=1.29$ [21] we have replotted our theoretical results for the crossover function F as a function of τ/τ_{cross} in Fig. 9. The data points in Fig. 9 are experimental results from [21] for the Onsager coefficient in EuO, where we have used $\tau_{\text{cross}}=0.119$ [24] for the reduced crossover temperature. The nonuniversal constant B for EuO, determined from (3.21), is $B_{\text{th}}=0.302$ meV, where we have taken the values for Λ and q_D from [24]: $\Lambda=7.1/5.1326$ meVÅ$^{5/2}$ and $q_D=0.147$ Å^{-1}. In order to fit with the experimental data we have used in Fig. 9 $B_{\text{exp}}=0.248$ meV, which is remarkably close to B_{th}. However, the most important conclusion to be drawn from Fig. 9 is, that there is agreement of experiment and theory without any adjustable parameter for the temperature variable. As can be seen from Fig. 6 of [21] our theoretical results agree also well with the longitudinal relaxation measurements of Kötzler et al. [17]. There are also experimental results by Kötzler et al. for EuS and several other nearly isotropic ferromagnets [18–20] showing qualitatively the same behaviour for the Onsager coefficient. A quantitative comparison of the numerical data of these experiments with our theory would be of great interest.

3.2.3 Relaxation time for hyperfine interaction experiments. In hyperfine interaction experiments one observes the nuclear relaxation rate due to the surrounding fluctuating electronic magnetic moments. The standard experiments are performed in the motional narrowing regime [22]. Then assuming a contact interaction $H(t)=A\ I\cdot S(t)$ between I the nuclear and S the electronic spins, the nuclear relaxation rate τ_R^{-1} is directly proportional to the (averaged) spin-autocorrelation time τ_c

$$\tau_c=\frac{1}{2}\int_{-\infty}^{+\infty}\mathrm{d}t\,\frac{1}{3}\sum_{\alpha}G^{\alpha\alpha}(\mathbf{r}=0,t), \tag{3.24}$$

where $G^{\alpha\alpha}(\mathbf{r},t)=\frac{1}{2}\langle\{S^{\alpha}(\mathbf{r},t),\,S^{\alpha}(0,0)\}\rangle$ is the spin autocorrelation function. With

$$G^{\alpha\alpha}(\mathbf{r},t)=\frac{1}{V_q}\int_{\text{BZ}}\mathrm{d}^3q\,\mathrm{e}^{\mathrm{i}\mathbf{q}\mathbf{r}}\int_{-\infty}^{+\infty}\mathrm{d}t\,\mathrm{e}^{\mathrm{i}\omega t}G^{\alpha\alpha}(\mathbf{q},\omega) \tag{3.25a}$$

and the fluctuation dissipation theorem between, which in the special case $\omega=0$ reduces to

$$G^{\alpha\alpha}(\mathbf{q},\omega=0)=2k_BT\frac{\chi^{\alpha}(q,g)}{\Gamma^{\alpha}(q,g)}, \tag{3.25b}$$

we find for the auto-correlation time

$$\tau_c=\frac{k_BT}{V_q}\int_{\text{BZ}}\mathrm{d}^3q\,\frac{1}{3}\sum_{\alpha}\frac{\chi^{\alpha}(q,g)}{\Gamma^{\alpha}(q,g)}. \tag{3.26}$$

The q-integration extends over the Brillouin zone (BZ), the volume of which is V_q. Introducing the scaling functions (3.9) and (3.11) (3.26) can be written as

$$\tau_c\propto 4\pi\int\mathrm{d}k\,k^{-z}\frac{1}{3}\sum_{\alpha}\frac{\hat{\chi}^{\alpha}(k\xi,kg^{-1/2})}{\gamma^{\alpha}(k\xi,kg^{-1/2})}. \tag{3.27}$$

If there were no dipolar interaction, one could extract the temperature dependence from the integral in (3.27) with the result $\tau_c\propto\xi^{z-1}$. We use this expression to define an effective dynamical exponent $z_{\text{eff}}(\tau)$, which depends on the reduced temperature τ by

$$\tau_c\propto\xi^{z_{\text{eff}}-1}.$$

In the presence of dipolar forces one finds after introducing polar coordinates as in Sect. 3.1

$$\tau_c=H\left(1+\frac{1}{g\xi^2}\right)^{(1-z)/2}\int_{r_0}^{\infty}\mathrm{d}r\,r^{-2+z}\frac{1}{3}\sum_{\alpha}\frac{\hat{\chi}^{\alpha}(r,\varphi)}{\gamma^{\alpha}(r,\varphi)}, \tag{3.28}$$

where $z=5/2$ and the nonuniversal constant H is given by

$$H=\frac{(k_BT)^2}{2\pi^5(\Lambda a^{-5/2})^3}(q_Da)^{3/2}. \tag{3.29}$$

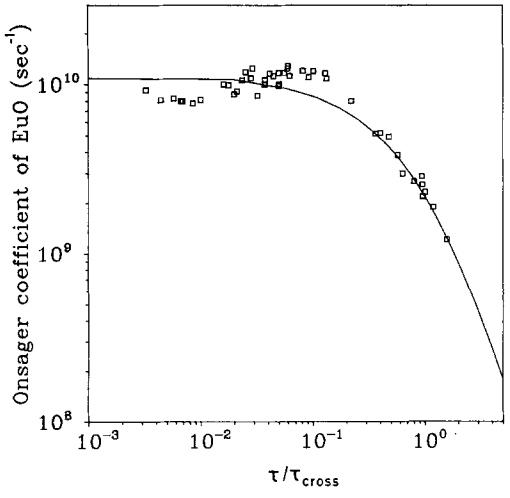

Fig. 9. Scaling function for the zero wave vector Onsager coefficient versus τ/τ_{cross} as explained in the text. The data points are experimental results from [21] for the Onsager coefficient in EuO

The lower cutoff r_0 is

$$r_0 = \frac{q_D}{q_{BZ}} \left[1 + \frac{1}{g\xi^2}\right]^{1/2}, \tag{3.30}$$

where q_{BZ} is the boundary of the Brillouin zone. In the critical region it can be neglected ($r_0 = 0$), since $q_{BZ} \gg q_D$ and the integrand in (3.28) is proportional to $r^{1/2}$ for small r. For very small ξ (outside the critical region) the cutoff reduces the autocorrelation time with respect to the critical value.

The autocorrelation time τ_c is a sum of two parts

$$\tau_c = (\tau_L + 2\tau_T)/3$$

which we call longitudinal and transverse relaxation times

$$\tau_L = H\left(1 + \frac{1}{g\xi^2}\right)^{-3/4} \int_{r_0}^{\infty} \mathrm{d}r\, r^{1/2} \frac{\hat{\chi}^L(r,\varphi)}{\gamma^L(r,\varphi)} \tag{3.31a}$$

$$\tau_T = H\left(1 + \frac{1}{g\xi^2}\right)^{-3/4} \int_{r_0}^{\infty} \mathrm{d}r\, r^{1/2} \frac{\hat{\chi}^T(r,\varphi)}{\gamma^T(r,\varphi)}. \tag{3.31b}$$

These two relaxation times are shown in Fig. 10 as functions of the scaling variable $(g^{1/2}\xi)^{-1}$, where we have neglected the lower cutoff r_0. As expected the longitudinal relaxation time is noncritical, whereas the transverse relaxation time diverges like $\tau_T \propto \xi$. This corresponds to an effective dynamical exponent $z_{\text{eff}} = 2$. If one leaves the dipolar critical region there is a crossover to the isotropic region, where both curves join and the relaxation times $\tau_L = \tau_T = \tau_c$ are characterised again by a simple power law $\tau_c \propto \xi^{3/2}$ corresponding to an effective dynamical exponent $z_{\text{eff}} = 2.5$.

Making the same approximations as in Sect. 3.2.2 with $\gamma = 1.38$ and $\tau_{\text{cross}} = 8.27 \cdot 10^{-3}$ for Fe [24], we

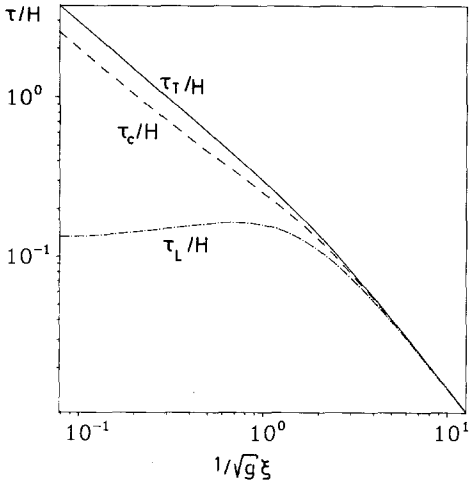

Fig. 10. Scaling functions for the longitudinal, transverse and averaged auto-correlation-time versus $(g^{1/2}\xi)^{-1}$

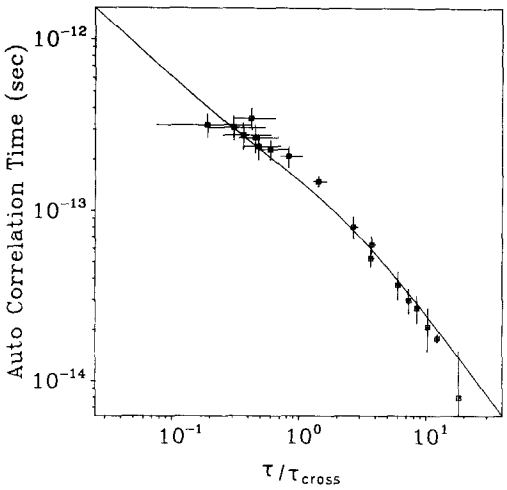

Fig. 11. Scaling function for the (averaged) auto-correlation-time versus τ/τ_{cross} as explained in the text. The data points are experimental results from [22] for the auto-correlation time of Fe

have replotted our theoretical result for the auto correlation time in Fig. 11 as a function of τ/τ_{cross}. The data points are experimental results for the spin-autocorrelation in ^{100}RhFe [22]. The only fit parameter in this figure is the nonuniversal scale H, which we have set to $H_{\text{exp}} = 6.0 \cdot 10^{-13}$ s. This value is quite close to the theoretical value $H_{\text{th}} = 7.55 \cdot 10^{-13}$ s, determined from (3.26) with $A = (1.14 * 94.0)/5.1326$ meV Å$^{5/2}$, $a = 2.87$ Å and $q_D = 0.147$ Å^{-1} [24]. The difference may be due to experimental uncertainties in the value of the coupling constant A. Furthermore (3.29) for the nonuniversal constant H may be plagued with minor inaccuracies in the same sense as B in Sect. 3.2.2. The main point however is that there is no adjustable parameter for the temperature variable. Hence we conclude, that the experimental data are well described within our theory.

4. Summary and conclusions

In this paper we have applied the mode coupling theory to study the critical dynamics of ferromagnets with both short range exchange interaction and long range dipolar interaction.

We start with the discussion of dipolar ferromagnets in the paramagnetic phase. On the basis of our theory we were able to explain the results of various experimental investigations on ferromagnets like EuO, EuS and Fe in a unified fashion. We have found that precisely at the critical temperature the crossover of the transverse width from $z = 2.5$ to $z = 2.0$ is shifted with respect to the static crossover to wave vectors smaller by almost one order of magnitude. This explains why up to now this crossover escaped detection

by neutron scattering experiments. Concerning the longitudinal width, experiments are still lacking. Our prediction is that the crossover from $z=2.5$ to an uncritical behaviour $z=0$ should be more pronounced in this case and, in contrast to the transverse width, it occurs in the immediate vicinity of the static crossover, characterized by q_D. Hence it should be detectable in the experimentally accessible wavevector region. The experimental results of Mezei on Fe at $T \geqq T_c$ taken at a series of temperatures show precisely the $(q\xi)^{-1}$ dependence of our theory.

Applying our theory to ESR and hyperfine interaction experiments we have found that in these cases the dynamical crossover is essentially determined by the static quantities. Up to minor uncertainties in the static crossover the theory is in excellent agreement with experiment. Concerning the hyperfine interaction experiments it would be interesting to devise experiments which allow to measure the longitudinal and transverse auto-correlation-time separately.

What seemed to be a rather contradictory and diverging field can be accomodated very naturally without adjustable parameters within our theory.

In the ordered phase we studied ferromagnets with short range interaction only. The results may serve as a reference for the study of the critical dynamics below T_c. More experimental data are needed for a comparison with the theory. We expect that in the immediate vicinity of T_c one will find experimentally similar dipolar crossover phenomena as above T_c.

If nessesary, the following refinements of the theory for the paramagnetic phase are possible. *(i)* One can compute the scaling functions and the linewidths directly from (3.5) and (3.7) without making the Lorentzian approximation [34]. *(ii)* One can use as static susceptibilities expressions more accurate than the Ornstein-Zernike susceptibility. Using the susceptibility of [35] a change of no more than several percent are found. *(iii)* One can perform a direct renormalization group analysis, which is in progress. The inclusion of dipole-dipole forces in the ferromagnetic phase is complicated because of two anisotropies (I) with respect to the direction of the magnetization (II) with respect to the wave vector.

This work has been supported by the German Federal Minister for Research and Technology (BMFT) under contract number 03-SC1TUM-0.

Note added in proof

The most interesting result of the solution of the complete mode coupling equations [34] concerns the transverse shape function. This becomes almost a Lorentzian. Thus it seems that dipolar forces are responsible also for this longstanding discrepancy between experiment and theories based solely on the short range exchange interaction

References

1. Resibois, P., Piette, C.: Phys. Rev. Lett. **24**, 514 (1970)
2. Aharony, A., Fisher, M.E.: Phys. Rev. B**8**, 3323 (1973)
3. Frey, E., Schwabl, F.: Phys. Lett. A**123**, 49 (1987)
4. Mori, H.: Progr. Theor. Phys. **33**, 423 (1965); **34** 399 (1965)
5. Kawasaki, K.: Progr. Theor. Phys. **39**, 285 (1968); Ann Phys. **61**, 1 (1970); In: Phase transitions and critical phenomena, Vol. 5a. Domb, C., Green, M. (eds.). New York, London: Academic Press 1976
6. Hubbard, J.: J. Phys. C**4**, 53 (1971)
7. Schwabl, F.: Z. Phys. **246**, 13 (1971)
8. Mazenko, G.F.: Phys. Rev. B**14**, 3933 (1976)
9. Iro, H.: Z. Phys. B – Condensed Matter **68**, 485 (1987)
10. Bhattacharjee, J.K., Ferrell, R.A.: J. Stat. Phys. **41**, 899 (1985)
11. Ma, S., Mazenko, G.F.: Phys. Rev. B**11**, 4077 (1975)
12. Sasvári, L.: J. Phys. C**10**, L633 (1977)
13. Collins, M.F., Minkiewicz, V.J., Nathans, R., Passell, L., Shirane, G.: Phys. Rev. **179**, 417 (1969)
14. Collins, M.F., Minkiewicz, V.J., Nathans, R., Shirane, G.: Phys. Rev. **182**, 624 (1969)
15. Dietrich, O.W., Als-Nielsen, J., Passell, L.: Phys. Rev. B**14**, 4923 (1976)
16. Mitchell, P.W., Cowley, R.A., Pynn, R.: J. Phys. C**17**, L875 (1984)
17. Kötzler, J., Scheithe, W., Blickhan, R.: Solid State Commun **26**, 641 (1978)
18. Kötzler, J., Kamleiter, G., Weber, G.: J. Phys. C**9**, L361 (1976)
19. Kötzler, J., von Philipsborn, H.: Phys. Rev. Lett. **40**, 790 (1978)
20. Kötzler, J., Scheithe, W.: J. Magn. Magn. Mater. **9**, 4 (1978)
21. Dunlap, R.A., Gottlieb, A.M.: Phys. Rev. B**22**, 3422 (1980)
22. Hohenemser, C., Chow, L., Suter, R.M.: Phys. Rev. B**26**, 5056 (1982)
23. Mezei, F.: Phys. Rev. Lett. **49**, 1096 (1982)
24. Mezei, F.: J. Magn. Magn. Mater. **45**, 67 (1984)
25. Mezei, F.: Physica **136**B, 417 (1986)
26. Böni, P., Shirane, G.: Phys. Rev. B**33**, 3012 (1986)
27. Borckmans, P., Walgraef, D., Dewel, G.: Physica A**91**, 411 (1977)
28. Riedel, E., Wegner, F.: Phys. Rev. Lett. **24**, 730 (1970)
29. Bruce, A.D., Kosterlitz, J.M., Nelson, D.R.: J. Phys. C**9**, 825 (1976)
30. Böni, P., Shirane, G., Bohn, H.G., Zinn, W.: J. Appl. Phys. **61**, 8 (1987)
31. Finger, W.: Physica **90**B, 251 (1977)
32. Finger, W.: Phys. Lett. A**60**, 165 (1977)
33. Raghavan, R., Huber, D.L.: Phys. Rev. B**14**, 1185 (1976)
34. Frey, E., Schwabl, F., Thoma, S.: Phys. Lett. A: (to be published)
35. Santos, M.A.: J. Phys. C**13**, 1205 (1980)

E. Frey, F. Schwabl
Physik-Department
Technische Universität München
-Theoretische Physik-
James-Franck-Strasse
D-8046 Garching bei München
Federal Republic of Germany